Stability of Na2Mg2Si2O7 and melting relations on the forsterite–jadeite join at pressures up to 22 GPa

Article *in* European Journal of Mineralogy · March 1997

CITATIONS
39

READS
125

2 authors, including:

Yu. A. Litvin
Russian Academy of Sciences
211 PUBLICATIONS **1,696** CITATIONS

SEE PROFILE

Eur. J. Mineral.
1997, **9**, 311-326

This paper was presented at the EMPG-VI
meeting in Bayreuth, Germany (April 1996)

Stability of $Na_2Mg_2Si_2O_7$ and melting relations on the forsterite-jadeite join at pressures up to 22 GPa

TIBOR GASPARIK[1,*)] and YURIY A. LITVIN[2)]

[1)]Center for High Pressure Research, Department of Earth and Space Sciences,
State University of New York at Stony Brook, Stony Brook, New York 11794, U.S.A.

[2)]Institute of Experimental Mineralogy, Russian Academy of Sciences,
142432 Chernogolovka, Moscow District, Russia

Abstract: Melting experiments on the forsterite-jadeite join (Mg_2SiO_4-$NaAlSi_2O_6$) were carried out at 4-22 GPa in a split-sphere anvil apparatus (USSA-2000). Forsterite-rich compositions produced below the solidus a divariant assemblage of forsterite, clinopyroxene, garnet, and $Na_2Mg_2Si_2O_7$ (NMS), with NMS being the solidus phase. The melting curves of NMS and Na_2MgSiO_4 (N2MS) were determined from 1 atm to 22 GPa. The results were used to solve the basic topology of the phase diagrams relevant to assemblages containing NMS and N2MS. It is expected that NMS is present in the Earth's mantle in nepheline-normative compositions due to the instability of nepheline at higher pressures. However, at pressures higher than 13 GPa, NMS-bearing assemblages could potentially form even at lower sodium contents more common in the mantle, and cause a major decrease in the temperatures of the anhydrous solidus in the transition zone (400-670 km). Such a decrease in the solidus temperatures is likely to have a profound effect on the evolution of the Earth's mantle in any scenario involving a magma ocean.

Key-words: forsterite-jadeite join, high-pressure experiments, melting relations, $Na_2Mg_2Si_2O_7$, multianvil press.

1. Introduction

Phase relations on the forsterite-jadeite (Fo-Jd) join are applicable to the classic problem of the origin of olivine tholeiites and alkali basalts. Yoder & Tilley (1962) demonstrated that the breakdown of the thermal divide between forsterite and albite and its replacement by a new thermal divide between enstatite and jadeite at high pressures is responsible for the change in composition of the basaltic melts from tholeiitic at lower pressures to alkaline at higher pressures. This reflects the depth of origin, which is shallow for the tholeiitic magmas, typically generated under the mid-ocean ridges, but greater for alkali basaltic magmas originating under the older and thicker oceanic lithosphere.

Melting relations on the Fo-Jd join were investigated by Windom & Boettcher (1981) at 2.8 GPa and are shown, with our modifications, in Fig. 1a. The stable assemblage below the solidus was reported to be forsterite and jadeite. Orthopyroxene replaced forsterite on the liquidus at higher jadeite contents, which confirmed the

*E-mail: gasparik@sbmp04.ess.sunysb.edu

0935-1221/97/0009-0311 $ 4.00

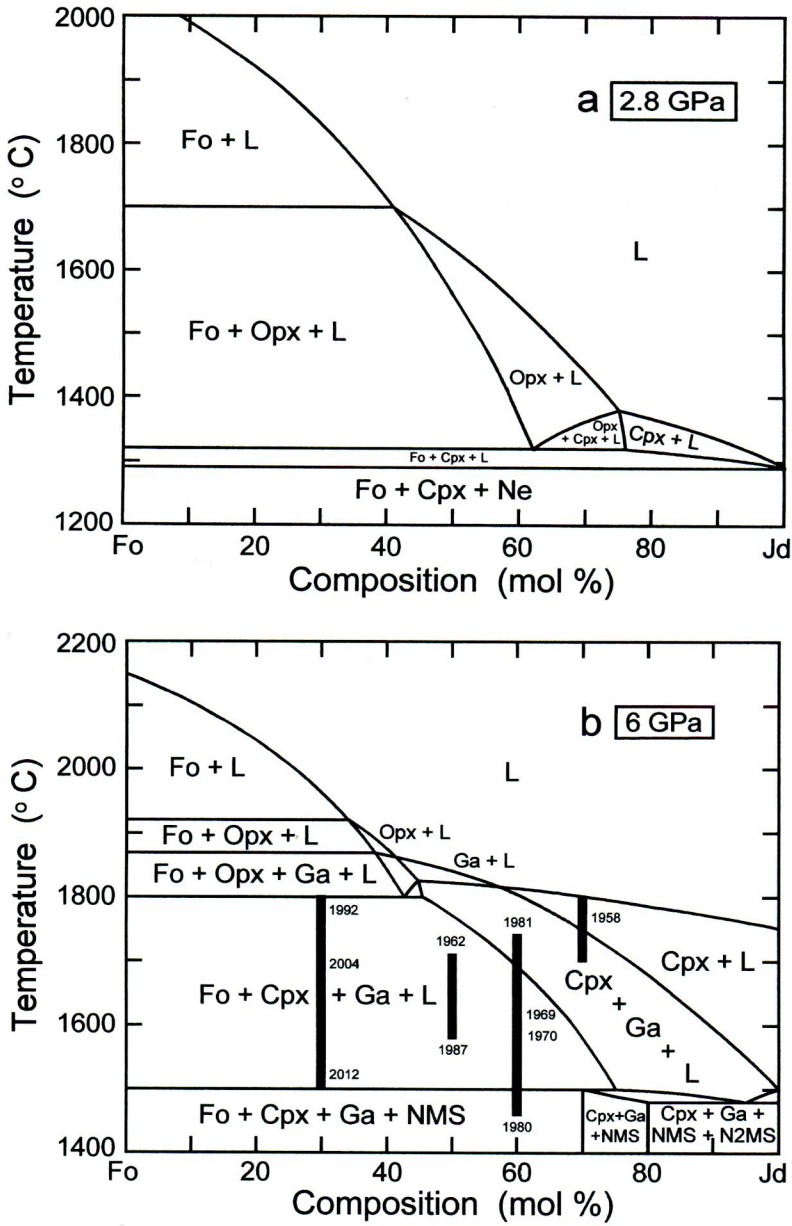

Fig. 1. Temperature-composition phase diagrams for the forsterite-jadeite join at (a) 2.8 GPa, modified after Windom & Boettcher (1981), and (b) 6 GPa, this study. Bars show the compositions and the temperature range explored by the experiments, assuming a temperature variation of 100°C in each sample. Numbers refer to experiments in Table 2. Symbols: Cpx = clinopyroxene, Fo = forsterite, Ga = garnet, L = liquid, Ne = nepheline, NMS = $Na_2Mg_2Si_2O_7$, N2MS = Na_2MgSiO_4, Opx = orthopyroxene.

previous observations of melting relations for similar compositions in the system forsterite-nepheline-silica by Kushiro (1965), and was documented later in more detail by Gupta *et al.* (1987). The resulting melting relations were consistent with the origin of alkali basalts by partial melting at the corresponding depth.

We decided to investigate the melting relations

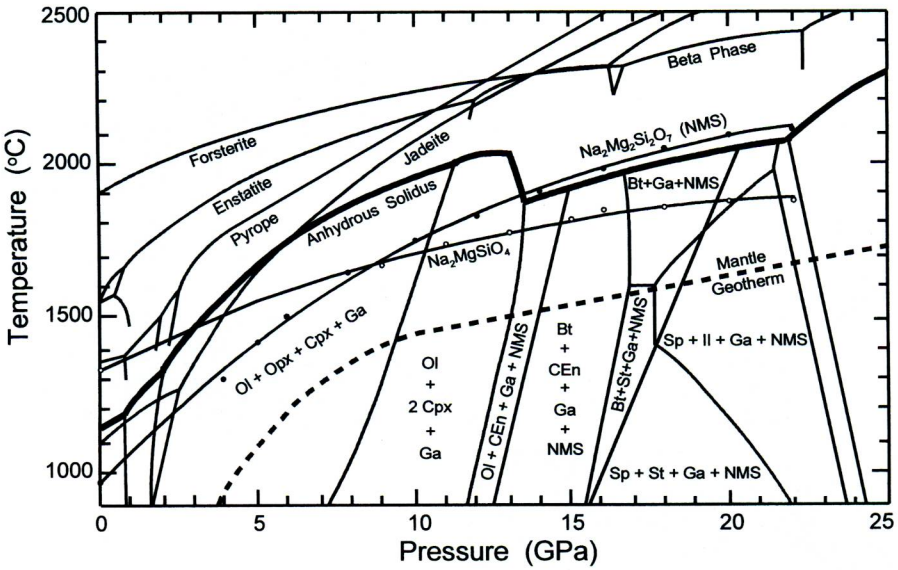

Fig. 2. Temperature-pressure phase diagram showing the proposed anhydrous solidus (heavy solid line). Also shown are the new melting curves with the location of experiments for the melting of NMS (dots) and N2MS (circles), and the previously determined melting curves of other simple compounds relevant to the melting relations on the forsterite-jadeite join (Litvin & Gasparik, 1993; Presnall & Gasparik, 1990; Presnall & Walter, 1993; Zhang & Herzberg, 1994b). Symbols: Bt = beta phase, CEn = clinoenstatite, Il = $MgSiO_3$ ilmenite, Ol = olivine, Sp = Mg_2SiO_4 spinel, St = stishovite.

on the Fo-Jd join at pressures higher than 2.8 GPa to determine the character of the partial melts originating at even greater depths than the alkali basaltic melts. Our preliminary experiments at 6 GPa showed indications that forsterite and jadeite reacted under subsolidus temperatures. The most obvious signs were the appearance of garnet and the change in the composition of clinopyroxene from pure jadeite to intermediate pyroxene containing a significant enstatite component in solution. Closer scrutiny revealed the presence of a sodium-rich phase with the composition $Na_2Mg_2Si_2O_7$ (NMS). A phase of this composition was previously observed at 1 atm (Botvinkin & Popova, 1937; Manuilova, 1937) but not at high pressures. Our preliminary observations suggested the possibility that this phase could be present in the Earth's mantle and was deemed worthy of further investigation.

Gasparik (1989, 1992) investigated the phase relations on the enstatite-jadeite (En-Jd) join at pressures between 6 and 22 GPa. The results suggested that these phase relations could potentially play an important role in deciphering the evolution of the upper mantle. Also reported was the occurrence of another sodium-rich phase, Na_2MgSiO_4 (N2MS), coexisting with Mg_2SiO_4 beta phase, pyroxene and garnet at 13.6-16 GPa. To verify and expand these observations, the investigation of the Fo-Jd join was extended to 22 GPa.

2. Experimental techniques

Experiments were conducted in a split-sphere anvil apparatus using three different sample assemblies. The 18/12 assembly (Litvin & Gasparik, 1993) was used in the pressure range of 4-6 GPa, the 10/5 assembly (Gasparik, 1989) was used at 8-16 GPa, and the 10/4 assembly (Gasparik, 1990) at 18-22 GPa. Due to the temperature gradients, the temperature in the 18 mm assembly varies from the temperature recorded by the thermocouple in the hot spot to about 100°C lower temperature in the cold end of the sample. The temperature gradients are even higher in the 10 mm assembly. The temperature recorded by the thermocouple is approximately the same as the temperature at the center of the sample, it is

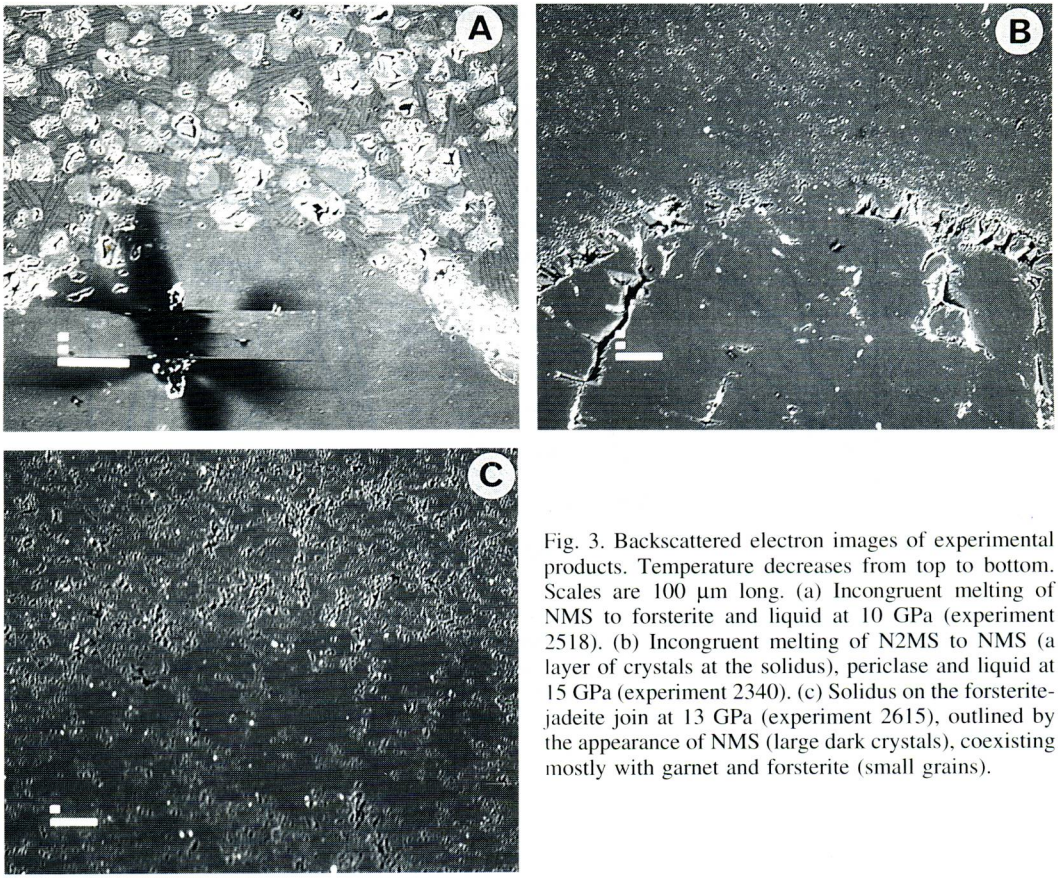

Fig. 3. Backscattered electron images of experimental products. Temperature decreases from top to bottom. Scales are 100 μm long. (a) Incongruent melting of NMS to forsterite and liquid at 10 GPa (experiment 2518). (b) Incongruent melting of N2MS to NMS (a layer of crystals at the solidus), periclase and liquid at 15 GPa (experiment 2340). (c) Solidus on the forsterite-jadeite join at 13 GPa (experiment 2615), outlined by the appearance of NMS (large dark crystals), coexisting mostly with garnet and forsterite (small grains).

about 50°C higher in the hot spot, and 150°C lower in the cold end of the sample. The details about the sample assemblies, temperature and pressure calibrations, and experimental procedures were given by Gasparik (1989, 1990) and Litvin & Gasparik (1993).

For the experiments on the Fo-Jd join, several starting materials with compositions $Fo_{30}Jd_{70}$, $Fo_{40}Jd_{60}$, $Fo_{50}Jd_{50}$ and $Fo_{70}Jd_{30}$ (mol.%) were prepared by mixing either gels or crystalline materials of end-member forsterite and jadeite compositions. Crystalline forsterite and jadeite were prepared from the same gels crystallized for 16 hours at 4 GPa in an anvil-with-hole apparatus (Litvin, 1991) at 1400°C for forsterite and 1200°C for jadeite. For the melting of $Na_2Mg_2Si_2O_7$ and Na_2MgSiO_4, stoichiometric mixes were prepared from high-purity Na_2CO_3, MgO and amorphous SiO_2, first decarbonated in air by slowly increasing the temperature from 400 to 800°C over a period of several hours, and then sintered at 800°C for 3 days. The starting materials were initially dried at 100°C and stored in a dessicator. After being loaded in rhenium capsules and placed inside the assemblies, they were fired under argon at 1000°C for 1 hour to assure anhydrous conditions. Only $Na_2Mg_2Si_2O_7$ was not fired with the assembly to avoid melting.

After the experiments, the samples, still inside their capsules, were mounted in epoxy. Polished mounts contained lengthwise sections of the samples. The samples were examined optically under microscope, and then analyzed by a Cameca electron microprobe. Wavelength-dispersive chemical analyses were obtained at 15 kV accelerating potential and 10 nA beam current, using enstatite for Mg and Si, albite for Na, and grossular for Al. The counting time on each element was only 10 seconds to minimize the loss of sodium.

Experimental products were usually well crystallized, with the crystal size typically exceeding 10 μm. This made possible to obtain high-quality microprobe analyses, as is evident from the

Table 1. Experimental conditions, results and compositions of phases from the melting of $Na_2Mg_2Si_2O_7$ and Na_2MgSiO_4.

Run #	t[a] (min)	P_g[b] (bar)	P_s (GPa)	T_s[c] (°C)	T_m[d] (°C)	Result[e]	Composition Na	Mg	Si	O
$Na_2Mg_2Si_2O_7$ (NMS)										
2639	6	400	4	1350	1300	NMS = Fo + L				
						NMS	1.923	1.984	2.026	7
						L	2.048	1.050	1.963	6
2565	6	450	5	1400		NMS	1.914	2.035	2.003	7
2632	6	450	5	1450	1420	NMS = Fo + L				
						NMS	2.029	1.915	2.034	7
						L	2.201	1.596	1.651	6
2556	6	500	6	1550	1500	NMS = Fo + L				
						NMS	1.937	2.034	1.998	7
						L	2.592	0.685	2.008	6
2555	6	114	8	1630	1650	NMS = Fo + L				
						NMS	1.859	1.949	2.060	7
						L	2.551	0.904	1.909	6
2518	6	160	10	1700	1750	NMS = Fo + L				
						NMS	1.876	1.968	2.047	7
						L	2.813	0.512	2.039	6
2561	6	226	12	1780	1830	NMS = L				
						NMS	1.778	2.037	2.036	7
						L	1.845	1.539	1.767	6
2563	6	320	14	1860	1910	NMS = L				
						NMS	1.713	2.041	2.050	7
						L	1.556	1.643	1.789	6
2564	6	500	16	1950	1990	NMS = Pc + L				
						NMS	1.908	2.050	1.997	7
						L	1.907	1.640	1.700	6
2571	4	462	18	2020	2060	NMS = Pc + L				
						NMS	1.903	2.017	2.014	7
						L	1.788	1.616	1.743	6
2578	6	560	20	2100	2100	NMS = Pc + L				
						NMS	2.019	1.965	2.011	7
						L	2.230	1.438	1.721	6
2597	6	710	22	2100	2110	NMS = Pc + L				
						NMS	1.920	1.974	2.032	7
						L	1.829	1.299	1.889	6
Na_2MgSiO_4 (N2MS)										
2378	6	136	9	1650	1670	N2MS = Pc + L				
						N2MS	1.987	0.999	1.003	4
						L	3.252	1.204	1.574	6
2365	3	190	11	1700	1740	N2MS = Pc + L				
						N2MS	1.996	0.990	1.006	4
						L	3.324	0.740	1.799	6
2358	6	270	13	1800	1780	N2MS = NMS + Pc + L				
						N2MS	1.958	0.993	1.012	4
						NMS	1.829	2.008	2.035	7
						L	3.376	0.715	1.785	6
2340	6	390	15	1800	1820	N2MS = NMS + Pc + L				
						N2MS	1.953	0.996	1.011	4
						NMS	1.854	2.039	2.015	7
						L	3.500	0.708	1.766	6
2369	6	500	16	1800	1850	N2MS = NMS + Pc + L				
						N2MS	1.972	1.009	1.002	4
						NMS	1.809	2.030	2.027	7
						L	3.426	0.882	1.701	6
2574	5	462	18	1850	1860	N2MS = NMS + Pc + L				
						N2MS	2.101	0.904	1.022	4
						NMS	2.005	1.990	2.004	7
						L	3.339	0.767	1.781	6
2610	6	560	20	1850	1880	N2MS = NMS + Pc + L				
						N2MS	2.002	0.921	1.034	4
						NMS	1.932	1.950	2.040	7
						L	3.566	0.699	1.750	6
2658	6	710	22	1850	1880	N2MS = NMS + Pc + L				

[a] Duration of experiments in minutes

[b] Gauge pressure (P_g x 1.096 = load in metric tons)

[c] Temperature recorded by the thermocouple

[d] Estimated melting temperature

[e] Symbols: Fo = forsterite, L = liquid, Pc = periclase

Compositions are reported as cations per 4, 6 and 7 oxygens for N2MS, liquid and NMS, respectively.

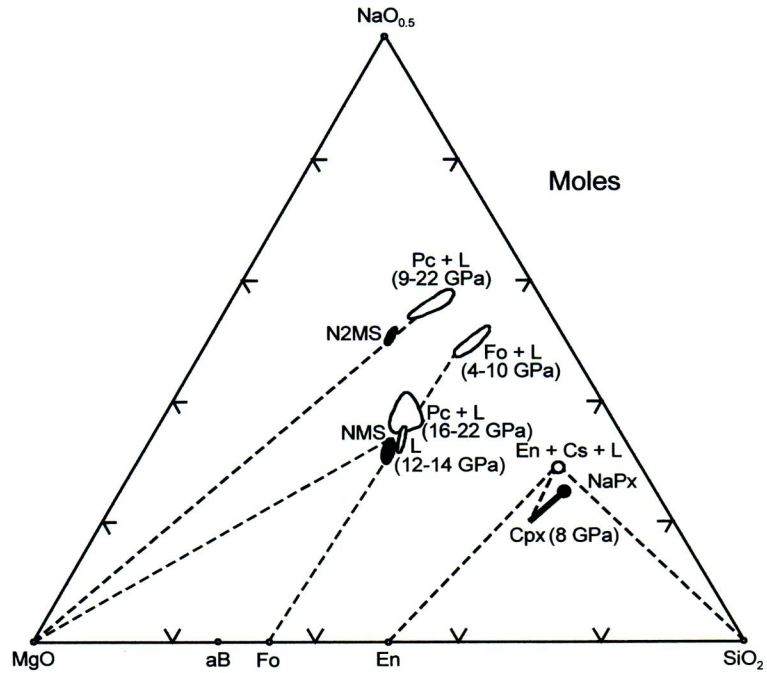

Fig. 4. Results from melting in the system $NaO_{0.5}$-MgO-SiO_2. Envelopes enclose the observed compositions of crystalline phases (solid) and liquids (open) coexisting on the solidus in the indicated pressure range. Labels include the products of incongruent melting. Melting of NaPx ($NaMg_{0.5}Si_{2.5}O_6$) is from Gasparik (1989); experiment 657, 1450°C/8 GPa. Symbols: aB = anhydrous phase B, Cs = coesite, En = enstatite, Pc = periclase.

excellent stoichiometry of the analyses of crystalline phases. The criteria for considering an analysis acceptable were the totals between 98 and 102 wt.% and, for pyroxene and garnet, the sums of cations per 6 oxygens between 3.98 and 4.02.

3. Experimental results

Melting curves of $Na_2Mg_2Si_2O_7$ and Na_2MgSiO_4

The melting curve of $Na_2Mg_2Si_2O_7$ was determined by 12 experiments from 1 atm to 22 GPa, with the melting temperatures ranging from 970 to 2110°C (Fig. 2). Melting was incongruent to forsterite and liquid at 4-10 GPa, congruent at 12-14 GPa, and incongruent to periclase and liquid at 16-22 GPa. The melting curve of Na_2MgSiO_4 was determined by nine experiments from 1 atm to 22 GPa, with the melting temperatures ranging from 1320 to 1880°C (Fig. 2). Melting was incongruent to periclase and liquid at 9-11 GPa, and incongruent to NMS, periclase and liquid at 13-22 GPa. In most experiments, the melting curve was located near the hot spot, allowing reliable estimates of the melting temperatures due to the low temperature gradient in that part of the sample. Usually, the melting curve could be easily identified as a sharp boundary following an isotherm in the sample (Fig. 3a, 3b). Melting temperatures at 1 atm were determined with uncertainties of ± 5°C by DTA (Litvin *et al.*, in prep.).

Table 1 includes the compositions of NMS, N2MS and coexisting liquids from the melting experiments at high pressures. NMS shows substantial nonstoichiometry, with vacancies in the Na and Mg sites. The content of Si is usually close to 2 per 7 oxygens, although small excess is commonly observed at higher pressures. N2MS is much closer in composition to the ideal formula. The compositions of liquids are higher in Na than the compositions of NMS and N2MS, which is consistent with the observed incongruent character of melting (Fig. 4).

Table 2. Conditions of melting experiments on the forsterite-jadeite join and the average compositions of phases.

Run #	Mix[a]	t[b] (min)	P_g[c] (bar)	P_s[d] (GPa)	T_s[e] (°C)	Phase[f]	An.[g]	Cations/6 oxygens Na	Mg	Al	Si	Sum
2040	A	495	400	4.0	1380	Fo + Cpx + Ga + L						
2026	B	120	400	4.0	1400	Fo + Cpx + L						
2022	B	120	400	4.0	1500	Fo + Cpx + L						
2037	A	190	426	4.5	1500	Cpx + L						
						L	4	1.018	1.110	0.571	1.762	4.461
						Cpx	5	0.329	1.177	0.625	1.860	3.991
2021	B	111	450	5.0	1500	Fo + Cpx + Ga + L						
2032	A	375	450	5.0	1500	Fo + Cpx + Ga + L						
						L	4	1.469	1.541	0.185	1.724	4.919
						Ga	2	0.120	1.334	0.930	1.605	3.989
						Cpx	4	0.735	0.512	0.748	2.000	3.995
2017	B	120	450	5.0	1600	Fo + Cpx + Ga + L						
						L	5	1.462	1.429	0.237	1.742	4.870
						Ga	2	0.057	1.415	0.957	1.560	3.989
						Cpx	15	0.759	0.439	0.798	1.992	3.988
1991	B	60	450	5.0	1680	Fo + Cpx + Ga + L						
						L	6	1.826	0.980	0.347	1.793	4.946
						Ga	4	0.202	1.247	0.925	1.631	4.005
						Cpx	7	0.741	0.487	0.785	1.983	3.996
						Fo	1	0	2.960	0.010	1.513	4.483
2010	A	250	475	5.5	1600	Fo + Cpx + Ga + L						
						L	4	2.025	1.288	0.238	1.671	5.222
						Cpx	4	0.768	0.421	0.801	1.997	3.987
						Fo	1	0.021	2.981	0.019	1.490	4.511
2002	A	130	475	5.5	1690	Fo + Cpx + Ga + L						
						L	5	1.105	0.956	0.515	1.859	4.435
						Ga	1	0.087	1.396	0.885	1.617	3.985
						Cpx	3	0.478	0.996	0.593	1.937	4.004
						Fo	1	0.012	2.957	0.018	1.505	4.492
1980	C	6	500	6.0	1560	Fo + Cpx + Ga + NMS						
2012	D	173	500	6.0	1600	Fo + Cpx + Ga + NMS						
						NMS	4	1.689	1.427	0.175	1.734	5.025
						Ga	2	0.074	1.459	0.912	1.568	4.013
						Cpx	3	0.822	0.295	0.875	1.990	3.982
						Fo	1	0	2.994	0	1.503	4.497
1970	E	6	500	6.0	1650	Fo + Cpx + Ga + L						
1969	C	6	500	6.0	1670	Fo + Cpx + Ga + L						
1987	B	124	500	6.0	1680	Fo + Cpx + Ga + L						
						L	6	1.810	0.827	0.392	1.839	4.868
						Ga	3	0.133	1.358	0.905	1.609	4.005
						Cpx	2	0.775	0.461	0.779	1.991	4.006
						Fo	1	0	3.011	0	1.494	4.505
2004	D	80	500	6.0	1700	Fo + Cpx + Ga + L						
1962	B	6	500	6.0	1710	Fo + Cpx + Ga + L						
1981	C	6	500	6.0	1740	Fo + Cpx + Ga + L						
1992	D	10	500	6.0	1800	Fo + Cpx + Ga + L						
1958	F	14	500	6.0	1800	Cpx + Ga + L						
2394	G	240	136	9.0	1700	Fo + Cpx + Ga + NMS + L (Solidus)						
					1750	L	17	1.590	1.056	0.367	1.799	4.812
					1700	Ga	3	0.072	1.437	0.925	1.569	4.003
					1700	Cpx	5	0.691	0.643	0.687	1.990	4.011
					1700	Fo	2	0.007	3.003	0.014	1.486	4.510
					1700	NMS	3	1.639	1.442	0.218	1.706	5.005
2532	G	250	190	11.0	1800	Fo + Cpx + Ga + NMS + L (Solidus)						
					1800	L	24	1.593	1.106	0.215	1.887	4.801
					1800	Ga	11	0.091	1.456	0.827	1.628	4.002
					1800	Cpx	8	0.564	0.904	0.533	2.006	4.007
					1800	Fo	2	0.041	2.950	0.021	1.499	4.511
					1800	NMS	5	1.676	1.505	0.163	1.706	5.050
2615	D	240	270	13.0	1850	Fo + Cpx + Ga + NMS						
					1900	Ga	4	0.173	1.416	0.647	1.763	3.999
					1850	Ga	6	0.151	1.447	0.689	1.722	4.009
					1850	Cpx	8	0.536	0.999	0.403	2.062	4.000
					1850	Fo	3	0.019	2.948	0.022	1.504	4.493
					1850	NMS	12	1.572	1.610	0.105	1.723	5.010
2386	G	240	294	13.5	1880	Cpx + Ga + NMS						
					1880	Ga	15	0.251	1.307	0.668	1.783	4.009
					1880	Cpx	7	0.684	0.683	0.615	2.025	4.007
					1880	NMS	16	1.586	1.555	0.130	1.728	4.999
2454	D	30	294	13.5	1900	Fo + Ga + NMS + L (Solidus)						
					1900	L	2	2.121	1.369	0.095	1.714	5.299
					1900	Ga	13	0.234	1.320	0.652	1.793	3.999
					1900	Fo	4	0.010	2.940	0.003	1.525	4.478
					1900	NMS	5	1.437	1.550	0.124	1.773	4.884

Table 2. (Continued)

Run #	Mix[a]	t[b] (min)	P_g[c] (bar)	P_s[d] (GPa)	T_s[e] (°C)	Phase[f]	An.[g]	Cations/6 oxygens Na	Mg	Al	Si	Sum
2424	D	240	500	16.0	1940	Bt + Ga + NMS + aB						
					1950	Ga	6	0.191	1.451	0.566	1.802	4.010
					1950	aB	13	0.061	3.362	0.069	1.252	4.744
					1940	Ga	1	0.254	1.335	0.613	1.808	4.010
					1940	Bt	5	0.038	2.919	0.037	1.503	4.497
					1940	NMS	6	1.541	1.643	0.076	1.736	4.996
2584	D	30	500	16.0	1950	Bt + Ga + NMS + aB						
					2000	Ga	4	0.197	1.427	0.559	1.817	4.000
					1960	aB	3	0.058	3.310	0.072	1.276	4.716
					1950	Ga	6	0.242	1.380	0.529	1.853	4.004
					1950	Bt	3	0.031	2.888	0.036	1.521	4.476
					1950	NMS	11	1.624	1.588	0.069	1.748	5.029
2590	D	15	462	18.0	2000	Bt + Ga + NMS + aB + L (Solidus)						
					2000	L	7	2.078	1.487	0.064	1.689	5.318
					2000	aB	5	0.065	3.361	0.062	1.257	4.745
					2000	Ga	8	0.284	1.289	0.600	1.834	4.007
					2000	Bt	2	0.038	2.899	0.036	1.514	4.487
					2000	NMS	2	1.638	1.695	0.067	1.692	5.092
2627	D	60	560	20.0	2000	Bt + Ga + NMS + Pc						
					2000	Pc	3	0.099	5.807	0.090	0.004	6.000
					2000	Ga	12	0.281	1.340	0.447	1.923	3.991
					2000	Bt	4	0.030	2.831	0.036	1.549	4.446
					2000	NMS	2	1.668	1.549	0.040	1.778	5.035
2645	D	40	710	22.0	2000	Ga + NMS + Pc						
					2100	Pc	5	0.146	5.734	0.128	0	6.008
					2100	Ga	7	0.282	1.395	0.397	1.934	4.008
					2000	Pc	5	0.102	5.821	0.080	0.004	6.007
					2000	Ga	5	0.388	1.223	0.409	1.984	4.004
					2000	NMS	3	1.514	1.675	0.033	1.759	4.981

[a] Bulk compositions (mol %): A = $Fo_{50}Jd_{50}$ (gel); B = $Fo_{50}Jd_{50}$ (cryst.); C = $Fo_{40}Jd_{60}$ (cryst.); D = $Fo_{70}Jd_{30}$ (cryst. Fo, Jd gel); E = $Fo_{40}Jd_{60}$ (gel); F = $Fo_{30}Jd_{70}$ (cryst.); G = $Fo_{50}Jd_{50}$ (cryst. Fo, Jd gel)

[b] Duration of experiments in minutes

[c] Gauge pressure (P_g x 1.096 = load in metric tons)

[d] Sample pressure

[e] Temperature recorded by the thermocouple in experiments at 4-6 GPa; estimated temperatures in the samples at 9-22 GPa for the first appearance of the subsolidus assemblage and of the analyzed phases

[f] Symbols: aB = anhydrous phase B, Bt = beta phase, Cpx = clinopyroxene, Fo = forsterite, Ga = garnet, Jd = jadeite, L = liquid, Pc = periclase

[g] The total number of analyses accepted from the given experiment for each phase

Experiments on the forsterite-jadeite join

Melting relations on the Fo-Jd join were investigated from 4 to 22 GPa. The experimental conditions and the average microprobe analyses of the phases are given in Table 2. Fig. 5 and Fig. 6 show the range of the observed compositions for crystalline phases and melts. The resulting Fo-Jd solidus can be approximated by the following Simon equation (Simon & Glatzel, 1929):

$$P(GPa) = 4 + \{[T(K)/1473]^{6.2} - 1\}.$$

Interpretation of the results at 4-6 GPa pressures was hampered by the difficulty in distinguishing the crystalline phases and the quenched melt in reflected light; the individual phases could be identified only by their composition. The presence of unreacted forsterite and jadeite was a reliable indicator of the subsolidus conditions. Forsterite and jadeite started reacting only in the close vicinity of the solidus. The first signs of reaction were the formation of intermediate clinopyroxene containing enstatite component in solution at the contact between jadeite and forsterite, and the appearance of isolated garnet grains. Because the temperature variation in the 18 mm assembly is around 100°C, some of the experiments with the crystalline starting material showed unreacted forsterite and jadeite in the cold end of the sample and significant reaction and melting in the hot spot.

The phase relations for the Fo-Jd join based on the results at 4-6 GPa are shown in Fig. 1b. Most of the experimental products consisted of clinopyroxene and forsterite, with minor garnet

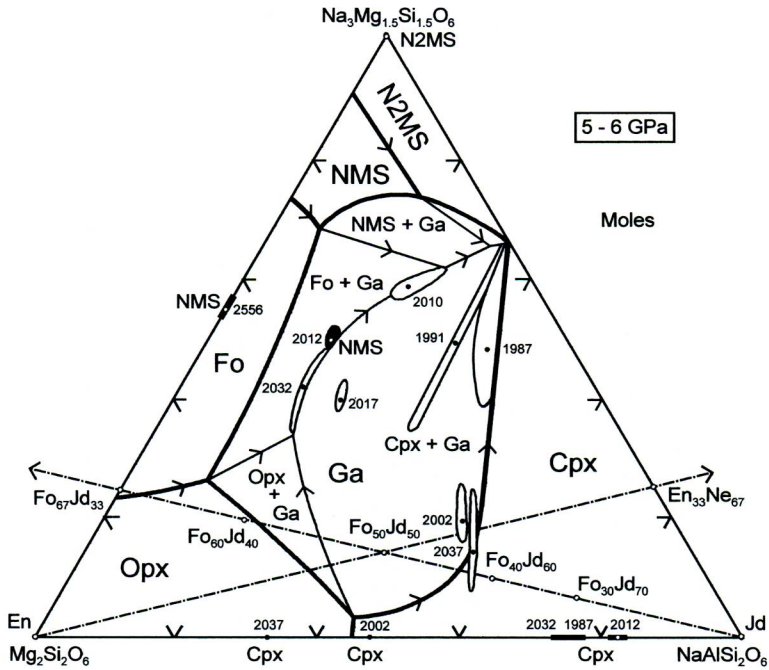

Fig. 5. Tentative melting relations in the pseudoternary system $Mg_2Si_2O_6$-$NaAlSi_2O_6$-$Na_3Mg_{1.5}Si_{1.5}O_6$ at 5-6 GPa projected from pyrope. Heavy boundaries outline the liquidus fields, thin cotectic lines indicate the compositions of melts coexisting with three phases. Envelopes enclose the observed range of compositions of melts (open) and crystals (solid), with the dots indicating averages. Numbers refer to experiments in Table 2. The phase boundaries not constrained by the data are hypothetical.

and quenched melt. However, some experiments with gels produced high concentrations of garnet in the hot spot, sometimes in the form of large round grains. NMS was present as small interstitial grains difficult to identify and analyze. Quenched melt was present either interstitially, or in some cases, offering the best opportunity for obtaining the composition, the melt segregated in small pools near the hot spot. The quenched melt could be identified visually from slightly different reflectance, or from slightly inferior polish in contrast to the better polish of the coexisting crystalline phases. The melt analyses are typical by their high sodium content, high cation total, and the lack of stoichiometry (Table 2). The analyses of melts obtained from experiments with run durations in minutes showed large variations in composition, apparently indicating that these short run durations were insufficient to reach equilibrium. However, the melt analyses from experiments lasting several hours plot in tight clusters and are considered to represent equilibrium compositions. The melt compositions plotted in Fig. 5 were calculated from microprobe analyses expressed in cations per 6 oxygens using the following scheme:

$X_{Jd} = Al$; $X_{N2MS} = (Na-Al)/3$; $X_{En} = 1-X_{Jd}-X_{N2MS}$.

The experimental products at 9-22 GPa were better equilibrated and the equilibration rates increased with pressure. Unreacted forsterite and jadeite were still present in the cold end of the sample at 9 GPa, but not at higher pressures. The solidus was often represented by a sharp boundary following an isotherm in the sample and indicating the first appearance of NMS (Fig. 3c). Good analyses of quenched melt were obtained at 9 and 11 GPa. However, at higher pressures, due to increased reaction rates, melt was replaced by garnet with a relatively low Na content in the duration of the experiments, as Na presumably migrated to the colder parts of the sample in response to the temperature gradient (see Lesher & Walker, 1988; Gasparik & Drake, 1995). Such

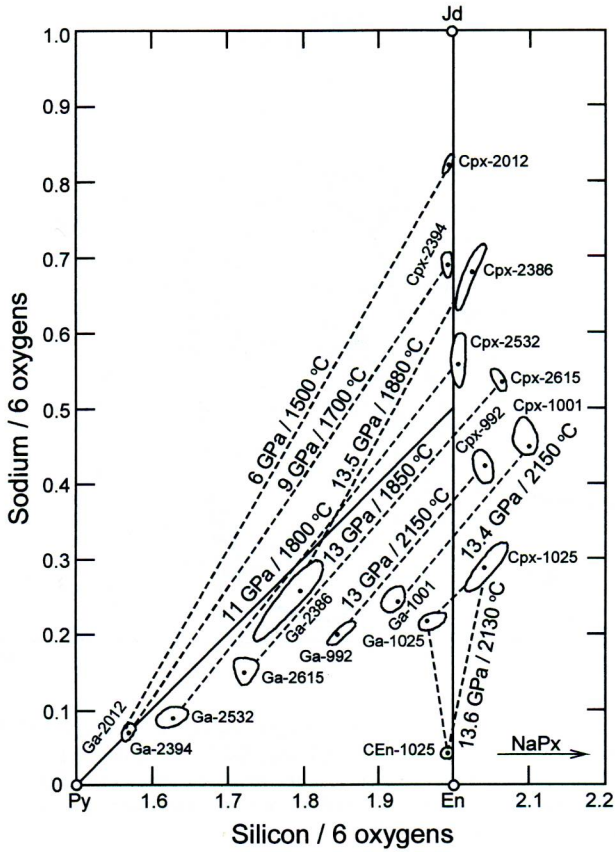

Fig. 6. Compositions of garnet and clinopyroxene coexisting at the solidus. Envelopes enclose the observed compositions, dots indicate averages. Experiments 992-1025 are from Gasparik (1992).

experiments usually did not yield melt compositions, although the presence of melt at the beginning of the experiments was suggested by the texture; it typically exhibited a sharp solidus between the fine matrix of the subsolidus assemblage containing NMS, and a much coarser garnet in the hot spot, where it replaced melt.

In the experiments at 16-18 GPa, garnet in the hot spot was accompanied also by anhydrous phase B, $Mg_{14}Si_5O_{24}$ (Finger *et al.*, 1989), while periclase joined garnet as the dominant phase at 20-22 GPa. The analyses of periclase revealed a significant coupled substitution of Na and Al. NMS was often present below the solidus as large crystals, apparently growing from the melt components migrating from the hot spot (Fig. 3c). In contrast to the experiments at 4-6 GPa, good analyses of NMS were easy to obtain at higher pressures. The analyses show the presence of Al in solution, and its content decreases with increasing pressure from 0.2 per 7 oxygens at 6 GPa to 0.04 at 22 GPa. The deficiency in Na and Mg and a slight excess of Si are similar to those observed in the experiments on melting of the Al-free NMS.

4. Discussion

The only prior experimental study of the Fo-Jd join was carried out by Windom & Boettcher (1981) at 2.8 GPa. While they report coexisting forsterite and jadeite below the solidus, they argue against the binary nature of the join because of the presence of enstatite component in clinopyroxene coexisting with melt. They suggest that the melt composition has to be nephe-

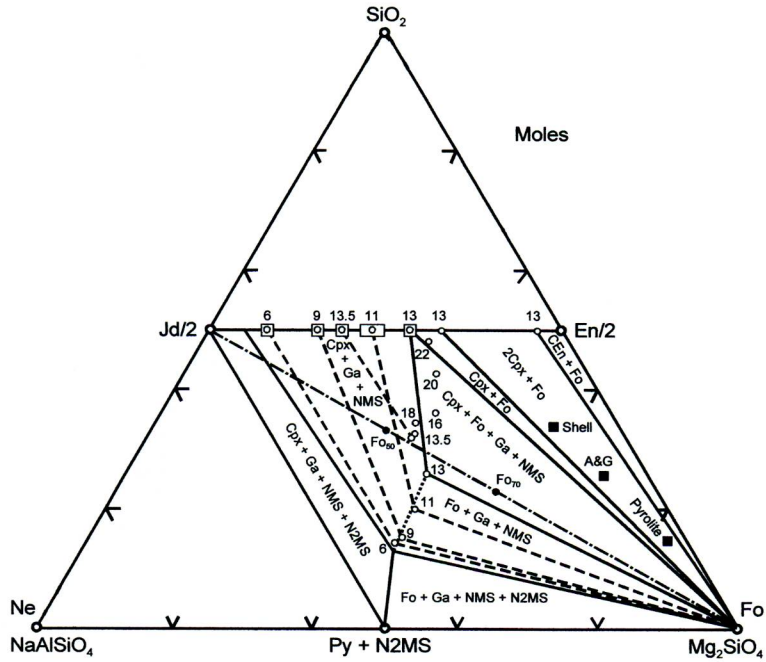

Fig. 7. Subsolidus phase relations in the system Fo-Ne-SiO_2 at 13 GPa (solid boundaries) and other pressures (dashed tie-lines), and at near solidus temperatures. Dotted line shows the trend with pressure of the piercing point corresponding to the intersection of the tie-line between coexisting garnet and NMS with the ternary plane. Examples of potential mantle compositions (solid squares) include pyrolite (Anderson, 1989, his Table 8-1), cosmic mantle (Anders & Grevesse, 1989) and shell (Gasparik, 1994).

line normative to compensate for the presence of enstatite in clinopyroxene. In contrast, our melt compositions at 4-6 GPa show an excess of Na over Al and clearly are different from the melt compositions inferred by Windom & Boettcher (1981). The missing Al is stored in our samples in garnet, while garnet was not reported by Windom & Boettcher (1981). Since jadeite coexisting with forsterite below the solidus also contains some enstatite component in solution, the subsolidus assemblage at 2.8 GPa has to include nepheline to remain on the Fo-Jd join. The most likely explanation for the difference between the results at 2.8 GPa and our observations is that nepheline is no longer stable at 4-6 GPa, and breaks down according to the following reaction (Gasparik *et al.*, 1996):

$$22\ Mg_2SiO_4 + 15\ NaAlSiO_4 + 5\ NaAlSi_2O_6 = 9\ Mg_3Al_2Si_3O_{12} + 10\ Na_2Mg_{1.7}Al_{0.2}Si_2O_7. \quad (1)$$

Nepheline was not observed in this study, thus its breakdown has to occur at pressures lower than 4 GPa. At such low pressures, the Na content of pyrope is negligible and the reaction (1) is close to univariant.

The Fo-Jd join belongs to the quaternary system Na_2O-MgO-Al_2O_3-SiO_2; such a system can have up to four coexisting phases. Fortunately, the observed melt compositions turned out to be very close to the plane $Mg_2Si_2O_6$-$NaAlSi_2O_6$-$Na_3Mg_{1.5}Si_{1.5}O_6$ (1.5 N2MS). This made possible to treat the system as ternary, resulting in a major simplification of the phase relations. The liquidus phase diagram for this pseudoternary system, inferred from our observations, is shown in Fig. 5. While the liquid compositions are fully expressed in this ternary diagram, the compositions of forsterite and garnet plot outside. To include these as well, the phase relations were projected to the ternary plane from pyrope. The position of the Fo-Jd join is evident from the following reaction:

$$6Mg_2SiO_4 + 3\ NaAlSi_2O_6 = 1.5\ Mg_3Al_2Si_3O_{12} + 3Mg_2Si_2O_6 + Na_3Mg_{1.5}Si_{1.5}O_6. \quad (2)$$

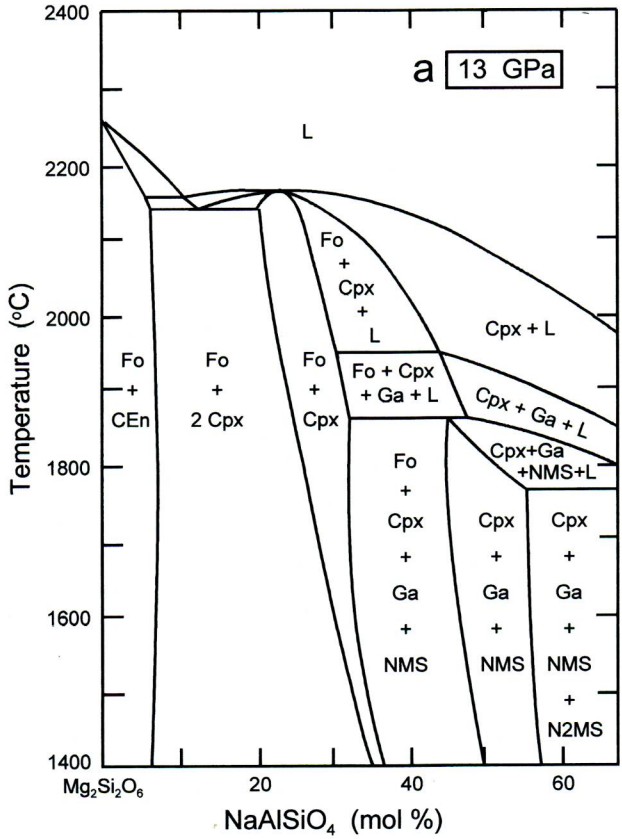

Fig. 8. Hypothetical temperature-composition phase diagrams for the enstatite-nepheline join at (a) 13 GPa and (b) 13.5 GPa.

Thus, the projection of the Fo-Jd join from pyrope intersects the join En-$Na_3Mg_{1.5}Si_{1.5}O_6$ at 75 mol.% En. This composition corresponds to $Fo_{67}Jd_{33}$.

We propose six liquidus surfaces: for forsterite, orthopyroxene, clinopyroxene, garnet, NMS and N2MS. Due to the quaternary nature of the system, the boundaries between any two liquidus surfaces are planes, which allow limited variation in the compositions of the liquids coexisting with two phases. The intersections of these planes then produce the cotectic lines showing the variation in the compositions of liquids coexisting with three phases: Opx + Cpx + Ga + L, Fo + Opx + Ga + L, Fo + Cpx + Ga + L, Fo + Ga + NMS + L, Cpx + Ga + NMS + L, Cpx + Ga + N2MS + L and Ga + NMS + N2MS + L. Most of the melts analyzed in this study were in equilibrium with forsterite, clinopyroxene and garnet and thus constrain the position of the corresponding cotectic line. In some experiments at higher temperatures (experiments #1987, 1991, 2002), the melt compositions had higher jadeite contents and apparently constrain the compositional plane for the liquids coexisting only with clinopyroxene and garnet. The remaining boundaries in Fig. 5 are hypothetical.

A preliminary phase diagram was constructed for the Fo-Jd join at 6 GPa (Fig. 1b) to be consistent with the data and with the diagram in Fig. 5. Most of the boundaries are again hypothetical and primarily constrained by our estimate of the solidus and by the melting curves of the end-member compounds enstatite, forsterite, pyrope, jadeite, NMS and N2MS (Fig. 2).

Fig. 7 shows the effect of pressure on the compositions of phases in the divariant assemblage Fo + Cpx + Ga + NMS in a familiar diagram

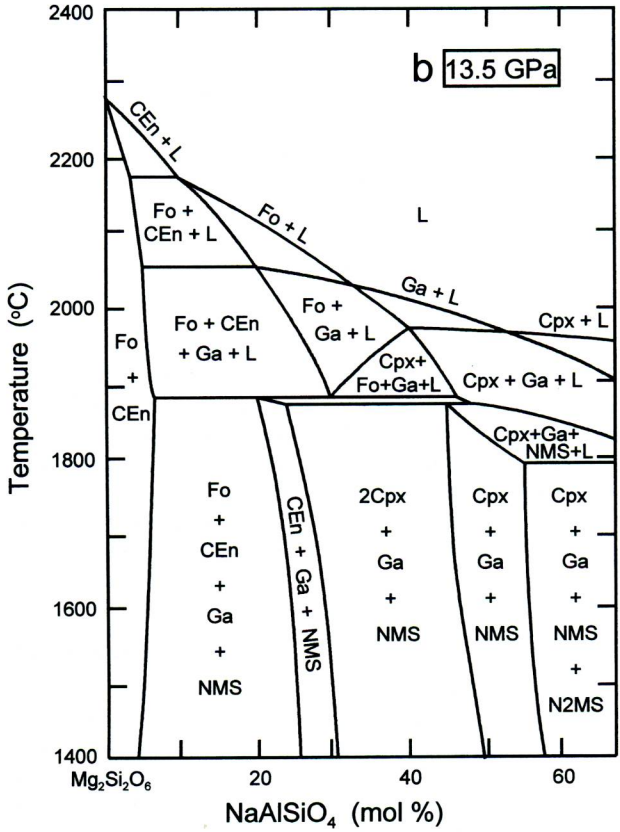

Fig. 8. (Continued)

forsterite-nepheline-silica, which represents the base of the basalt tetrahedron (Yoder & Tilley, 1962). In this diagram, only the compositions of forsterite and clinopyroxene can be shown directly, while the compositions of garnet and NMS are represented by a piercing point where the tie-line between garnet and NMS intersects the ternary plane. At the lowest pressures, where the composition of garnet is very close to pyrope, the position of this piercing point can be approximated with a modified version of reaction (1):

$$22\ Mg_2SiO_4 + 20\ NaAlSiO_4 + 5\ SiO_2 = 9\ Mg_3Al_2Si_3O_{12} + 10\ Na_2Mg_{1.7}Al_{0.2}Si_2O_7. \quad (3)$$

Compositions with lower silica contents or higher nepheline contents in the norm than this piercing point produce assemblages containing N2MS.

The piercing points in Fig. 7 were calculated using the observed compositions of garnet and NMS from Table 2 and Fig. 6. With increasing pressure, the piercing points and the compositions of coexisting jadeitic clinopyroxene move in the general direction towards enstatite. The piercing point reaches the Fo-Jd join between 13 and 13.5 GPa. The most enstatite-rich jadeitic clinopyroxene was found at 13 GPa, still in the divariant assemblage with Fo + Ga + NMS. At 13.5 GPa, the compositions on the Fo-Jd join can produce only 3-phase assemblages of either Fo + Ga + NMS or Cpx + Ga + NMS. The position of the piercing point does not change significantly between 13.5 and 18 GPa. The observed displacement from the Fo-Jd join at 16-18 GPa apparently reflects the presence of anhydrous B as the product of incongruent melting. However, the piercing point approaches the En-Jd join at 20-22 GPa due to the stabilization of periclase in a divariant assemblage with beta phase, garnet and NMS. Beta phase was not observed at 22 GPa and the garnet composition was very close

to the En-Jd join. Hence, at 22 GPa or a slightly higher pressure, the composition $Fo_{70}Jd_{30}$ fully transforms to garnet and periclase.

While the enstatite content of jadeitic clinopyroxene in the divariant assemblage with Fo + Ga + NMS increases with increasing pressure, from about 20 mol.% at 6 GPa to 60 % at 13 GPa, it decreases with pressure in another divariant assemblage with Fo + CEn (clinoenstatite), which is produced in more enstatite-rich compositions (Gasparik, 1992). Thus, the field of coexisting jadeitic clinopyroxene and forsterite, located between the two divariant fields, narrows with increasing pressure. At a pressure between 13 and 13.5 GPa, jadeitic clinopyroxene reacts with forsterite, producing a new divariant assemblage Fo + CEn + Ga + NMS. The melting in this assemblage is controlled by the melting of NMS and occurs at much lower temperatures than the melting in the assemblage Fo + 2Cpx. Hence, a major decrease in the solidus temperatures is suggested by the observed phase relations on the Fo-Jd and En-Jd joins between the pressures of 13 and 13.5 GPa.

Since the Fo-Jd join provides only the compositions of phases in the 4-phase assemblage Fo + Cpx + Ga + NMS, and the En-Jd join gives only the compositions of two coexisting pyroxenes, it is necessary to consider the phase relations in the ternary system En-Jd-Fo to fully describe the expected decrease in the solidus temperatures. Fig. 8 shows two hypothetical phase diagrams for the enstatite-nepheline (En-Ne) join, which cuts through the En-Jd-Fo system. At 13 GPa, the trivariant field of forsterite and clinopyroxene, which forms a thermal divide, is already very narrow, as it is squeezed out with increasing pressure by the two divariant fields: Fo + 2Cpx from the Mg-rich side, and Fo + Cpx + Ga + NMS from the Na-rich side. Melting experiments on the En-Jd join suggest that the melting of Fo + 2Cpx occurs at the relatively high temperatures in excess of 2100°C (Gasparik, 1992). The melting in the Na-rich compositions is controlled by the melting of NMS and occurs at much lower temperatures, which are up to 300°C lower than the melting temperatures of the forsterite-clinopyroxene thermal divide. At 13.5 GPa, the field of Fo + Cpx is eliminated and replaced by CEn + Ga + NMS. The solidus temperatures are now controlled by the melting of NMS even in the Mg-rich compositions common in the Earth's mantle. Hence, the solidus temperature decreases from 2140°C at 13 GPa, corresponding to the eutectic in the assemblage Fo + 2Cpx, to 1880°C at 13.5 GPa for the peritectic in the assemblage Fo + CEn + Ga + NMS.

The proposed anhydrous solidus is shown in Fig. 2. At pressures below 13 GPa, the solidus phase is clinopyroxene, and the solidus temperatures are similar to those observed in numerous melting studies with natural compositions expected in a peridotitic mantle (*e.g.* Zhang & Herzberg, 1994a). Between 13 and 13.5 GPa, the thermal divide between forsterite and clinopyroxene breaks down, producing clinoenstatite, garnet and liquid. NMS crystallizes from this liquid on a solidus which is about 250°C lower in temperature than the solidus at 13 GPa. In more complex mantle compositions, this temperature decrease is expected to be reduced to about 150°C, primarily due to the effect of iron on lowering the temperature of the peridotite solidus (*e.g.* Herzberg *et al.*, 1990).

5. Implications for the Earth's mantle

NMS-bearing assemblages are expected to form in the Earth's mantle from nepheline normative compositions at the pressures at which nepheline is no longer stable. Partial melting of the NMS-bearing assemblages at 4-6 GPa produces melts which lie to the N2MS-rich side of the Fo-Jd join (Fig. 5). These melts are unusual by their Na/Al ratios much higher than unity. In contrast, the nepheline-normative melts produced at lower pressures should have the Na/Al ratio close to unity, because the variation in the relative proportions of Na and Al is restricted by the stoichiometry of the Na-bearing phases, such as albite, nepheline and jadeite. Although, these melts can also be slightly peralkaline, due to the presence of a minor Mg-Tschermak component ($MgAl_2SiO_6$) in orthopyroxene (Gupta *et al.*, 1987), the stabilization of garnet with NMS allows for the first time the full decoupling of Na from Al in mantle processes. Hence, the partial melts generated at even greater depths than the alkali basaltic magmas will again have a unique signature reflecting the melting of NMS in the source region. It is possible that such melts are responsible for the alkaline volcanism associated with the rifting of thick continental lithosphere.

The proposed major decrease in the temperatures of the anhydrous mantle solidus at pressures higher than 13 GPa should have a profound effect

on the evolution of the Earth's mantle in any scenario involving a magma ocean. While the presence of Ca in more complex mantle compositions is likely to stabilize clinopyroxene to higher pressures, the proposed phase relations in the Ca-free system suggest the presence of a 5-phase divariant assemblage of Fo + 2Cpx + Ga + NMS in Ca-poor compositions. Due to the relatively low solidus temperatures of this assemblage, fractionation would tend to produce such Ca-poor compositions.

Crystallization of a magma ocean is expected to start with the development of a perched septum at depths less than 400 km. The septum, composed primarily of olivine and clinopyroxene, would form a barrier separating the magma ocean in the transition zone from the region above the septum. Subsequent fractionation of this deeper magma ocean could remove most of Ca by flotation of clinopyroxene, and possibly Al by gravitational settling of garnet. The residual transition zone would become enriched in volatile and incompatible elements, including Na, K and Fe, because this was the last region of the mantle crystallizing from the magma ocean. The proposed Na enrichment and low Ca and Al contents of the residual transition zone are consistent with the composition of an inclusion in diamond reported by Wang & Sueno (1996).

6. Conclusions

We have carried out the first preliminary experimental and theoretical investigation of melting relations on the Fo-Jd join at 4-22 GPa and solved the basic topology of the phase diagrams relevant to assemblages containing new mantle phases, NMS and N2MS. These phases are expected to form in the Earth's mantle instead of nepheline at pressures higher than the stability of nepheline. NMS should be present in the mantle in nepheline-normative compositions, while the compositions producing N2MS are probably rare.

The determined melting temperatures of NMS and N2MS are lower than the melting temperatures of other anhydrous mantle phases. Thus, the NMS-bearing assemblages will be among the first to melt, starting with NMS as the solidus phase. In particular, the low melting temperatures of NMS at pressures less than 3 GPa minimize the potential occurrence of NMS in xenoliths. Since micas or amphiboles could easily fill the role of NMS, the absence of H_2O is, apparently, also an important condition for the stability of NMS in the mantle, suggesting why NMS has not been observed in metamorphic rocks.

The NMS-bearing assemblages are potentially more common in the transition zone, provided that the phase relations in the system Na_2O-MgO-Al_2O_3-SiO_2 are applicable to chemically more complex mantle compositions. The corresponding decrease in the solidus temperatures of the transition zone would favor the formation of an Na-rich and Ca-poor layer in the final stages of crystallization of a magma ocean.

The present results did not explain the occurrence of N2MS reported by Gasparik (1989) at 1450°C and 15.2-16 GPa (experiments #380 and 389). It is possible that NMS is stable only near the solidus and breaks down at lower temperatures to N2MS and $Mg_4Si_4O_{12}$ garnet. The occurrence of N2MS reported by Gasparik (1992) at 1850°C and 13.6 GPa (experiment #1020) apparently represents quenched melt, since the experimental temperature was higher than the presently determined melting of N2MS.

Acknowledgements: This study was partially funded by the National Science Foundation grant EAR-9303865 to T. Gasparik. The visit of Yu. A. Litvin in Stony Brook and the high-pressure experiments were jointly supported by the National Science Foundation Science and Technology Center for High Pressure Research (EAR-8920239) and the University at Stony Brook.

References

Anders, E. & Grevesse, N. (1989): Abundances of the elements: Meteoritic and solar. *Geochim. Cosmochim. Acta*, **53**, 197-214.

Anderson, D.L. (1989) Theory of the Earth. Blackwell Scientific Publications, Boston Oxford London Edinburgh Melbourne, 366 p.

Botvinkin, O.K. & Popova, T.A. (1937): The melting diagram of the system Na_2SiO_3-Mg_2SiO_4-SiO_2 (in Russian). Trans. Second Conf. Exp. Mineral. Petrol., 7-10 May 1936, Acad. Sci. USSR, Moscow-Leningrad, 87-93.

Finger, L.W., Ko, J., Hazen, R.M., Gasparik, T., Hemley, R.J., Prewitt, C.T. & Weidner, D.J. (1989): Crystal chemistry of phase B and an anhydrous analogue: implications for water storage in the upper mantle. *Nature*, **341**, 140-142.

Gasparik, T. (1989): Transformantion of enstatite-diop-

side-jadeite pyroxenes to garnet. *Contrib. Mineral. Petrol.*, **102**, 389-405.

— (1990): Phase relations in the transition zone. *J. Geophys. Res.*, **95**, 15751-15769.

— (1992): Enstatite-jadeite join and its role in the Earth's mantle. *Contrib. Mineral. Petrol.*, **111**, 283-298.

— (1994): Mineral and chemical composition of the Earth's upper mantle. *Eos Trans. AGU*, Spring Meet. Suppl., **75**, 192-193.

Gasparik, T. & Drake, M.J. (1995): Partitioning of elements among two silicate perovskites, superphase B, and volatile-bearing melt at 23 GPa and 1500-1600°C. *Earth Planet. Sci. Lett.*, **134**, 307-318.

Gasparik, T., Dawkins, C.D., Litvin, Yu.A. (1996): Stability of $Na_2Mg_2Si_2O_7$ - the true solidus phase in Na-bearing olivine-normative mantle. *Terra Abs.*, Sixth Inter. Symp. Exp. Mineral. Petrol. Geochem., Bayreuth, Germany, **8**, 19-20.

Gupta, A.K., Green, D.H., Taylor, W.R. (1987): The liquidus surface of the system forsterite-nepheline-silica at 28 kb. *Amer. Jour. Sci.*, **287**, 560-565.

Herzberg, C., Gasparik, T., Sawamoto, H. (1990): Origin of mantle peridotite: Constraints from melting experiments to 16.5 GPa. *J. Geophys. Res.*, **95**, 15779-15803.

Kushiro, I. (1965): The liquidus relations in the systems forsterite-$CaAl_2SiO_6$-silica and forsterite-nepheline-silica at high pressures. *Carnegie Inst. Wash. Yearb.*, **64**, 103-109.

Lesher, C.E. & Walker, D. (1988): Cumulate maturation and melt migration in a temperature gradient. *J. Geophys. Res.*, **93**, 10295-10311.

Litvin, Yu.A. (1991): Physico-chemical studies of melting of materials from the Deep Earth (in Russian). Nauka, Moscow, 312 p.

Litvin, Yu.A. & Gasparik, T. (1993): Melting of jadeite to 16.5 GPa and melting relations on the enstatite-jadeite join. *Geochim. Cosmochim. Acta*, **57**, 2033-2040.

Manuilova, N.S. (1937): Crystalline phases in the system Na_2O-MgO-SiO_2. Trans. Second Conf. Exp. Mineral. Petrol., 7-10 May 1936, Acad. Sci. USSR, Moscow-Leningrad, 96-101.

Presnall, D.C. & Gasparik, T. (1990): Melting of enstatite ($MgSiO_3$) from 10 to 16.5 GPa and the forsterite (Mg_2SiO_4)-majorite ($MgSiO_3$) eutectic at 16.5 GPa: Implications for the origin of the mantle. *J. Geophys. Res.*, **95**, 15771-15777.

Presnall, D.C. & Walter, M.J. (1993): Melting of forsterite, Mg_2SiO_4, from 9.7 to 16.5 GPa. *J. Geophys. Res.*, **98**, 19777-19783.

Simon, F.E. & Glatzel, G. (1929): Remarks on the fusion-pressure curve. *Z. Anorg. Allg. Chemie*, **178**, 309-316.

Wang, W. & Sueno, S. (1996): Discovery of a NaPx-En inclusion in diamond: possible transition zone origin. *Min. J.*, **18**, 9-16.

Windom, K.E. & Boettcher, A.L. (1981): Phase relations for the joins jadeite-enstatite and jadeite-forsterite at 28 kb and their bearing on basalt genesis. *Amer. Jour. Sci.*, **281**, 335-351.

Yoder, H.S.Jr. & Tilley, C.E. (1962): Origin of basalt magmas: An experimental study of natural and synthetic rock systems. *J. Petrol.*, **3**, 342-532.

Zhang, J. & Herzberg, C. (1994a): Melting experiments on anhydrous peridotite KLB-1 from 5.0 to 22.5 GPa. *J. Geophys. Res.*, **99**, 17729-17742.

—, —(1994b): Melting of pyrope, $Mg_3Al_2Si_3O_{12}$, at 7-16 GPa. *Am. Mineral.*, **79**, 497-503.

Received 3 May 1996
Modified version received 9 September 1996
Accepted 6 November 1996